

Polymyxin B-Polysaccharide Polyion Nanocomplex with Improved Biocompatibility and Unaffected Antibacterial Activity for Acute Lung Infection Management

Mengying Chai, Yifan Gao, Jun Liu, Yongyan Deng, Dengfeng Hu, Qiao Jin,* and Jian Ji

The decade-old antibiotic, polymyxin B (PMB), is regarded as the last line defense against gram-negative “superbug.” However, the serious nephrotoxicity and neurotoxicity strongly obstruct further application of this highly effective antibiotic. Herein, a charge switchable polyion nanocomplex exhibiting pH-sensitive property is proposed to deliver PMB which is expected to improve the biosafety of PMB on the premise of retaining excellent antibacterial activity. The polyion nanocomplex is prepared through electrostatic interaction of positively charged PMB and negatively charged 2,3-dimethyl maleic anhydride (DA) grafted chitoligosaccharide (CS). The negative charge of CS-DA will convert to positive due to the hydrolysis of amide bonds in acidic infectious environment, leading to the disassembly of CS-DA/PMB nanocomplex and release of PMB. CS-DA/PMB nanocomplex does not show significant toxicity to mammalian cells while retaining excellent bactericidal capability equivalent to free PMB. The nephrotoxicity and neurotoxicity of CS-DA/PMB dramatically decrease compared to free PMB. Moreover, CS-DA/PMB nanocomplex exhibits superior bactericidal activity against *Pseudomonas aeruginosa* in an acute lung infection mouse model. The pH-sensitive polyion nanocomplexes may provide a new way to reduce the side effects of highly toxic antibiotics without reducing their intrinsic antibacterial activity, which is the key factor to achieve extensive in vivo clinical applications.


The increasing number of drug-resistant pathogenic bacteria has caused a global threat to human health.^[1,2] According to the report from World Health Organization (WHO) in 2017, antibiotic resistance kills about 700 000 people each year worldwide under estimate, and the number will rise to 10 million by 2050 unless new interventions are developed.^[3] WHO also ranked three carbapenem-resistant pathogens (*Pseudomonas aeruginosa*, *Acinetobacter baumannii*, and *Enterobacteriaceae*) as the most dangerous pathogens that brought serious threats to public health. These gram-negative bacteria can induce a variety of common diseases such as pneumonia, intra-abdominal,

urinary tract, skin, and soft tissue infections.^[4–7] Thus, there is an urgency to develop new strategies for alternative antibacterial treatments. Among various new strategies developed for antimicrobial treatment, an “old-fashioned” antibiotic, polymyxin B (PMB), regains the attention as it shows excellent bactericidal against gram-negative bacteria.^[8,9] The drug can rapidly eradicate pathogens by interacting with the lipopolysaccharide of the outer membrane in gram-negative bacteria due to their amphiphilic and cationic nature.^[10,11] However, one safety concern is the nephrotoxicity and neurotoxicity occurring during the systemic polymyxin therapy, which strongly limits the clinical applications of polymyxins.^[12,13] For instance, injection of high-dose polymyxin may cause kidney damage and nervous system dysfunction in many cases.^[14–16] Hence, there is an emergency to find a strategy to minimize the toxicity of polymyxin with effective dose.

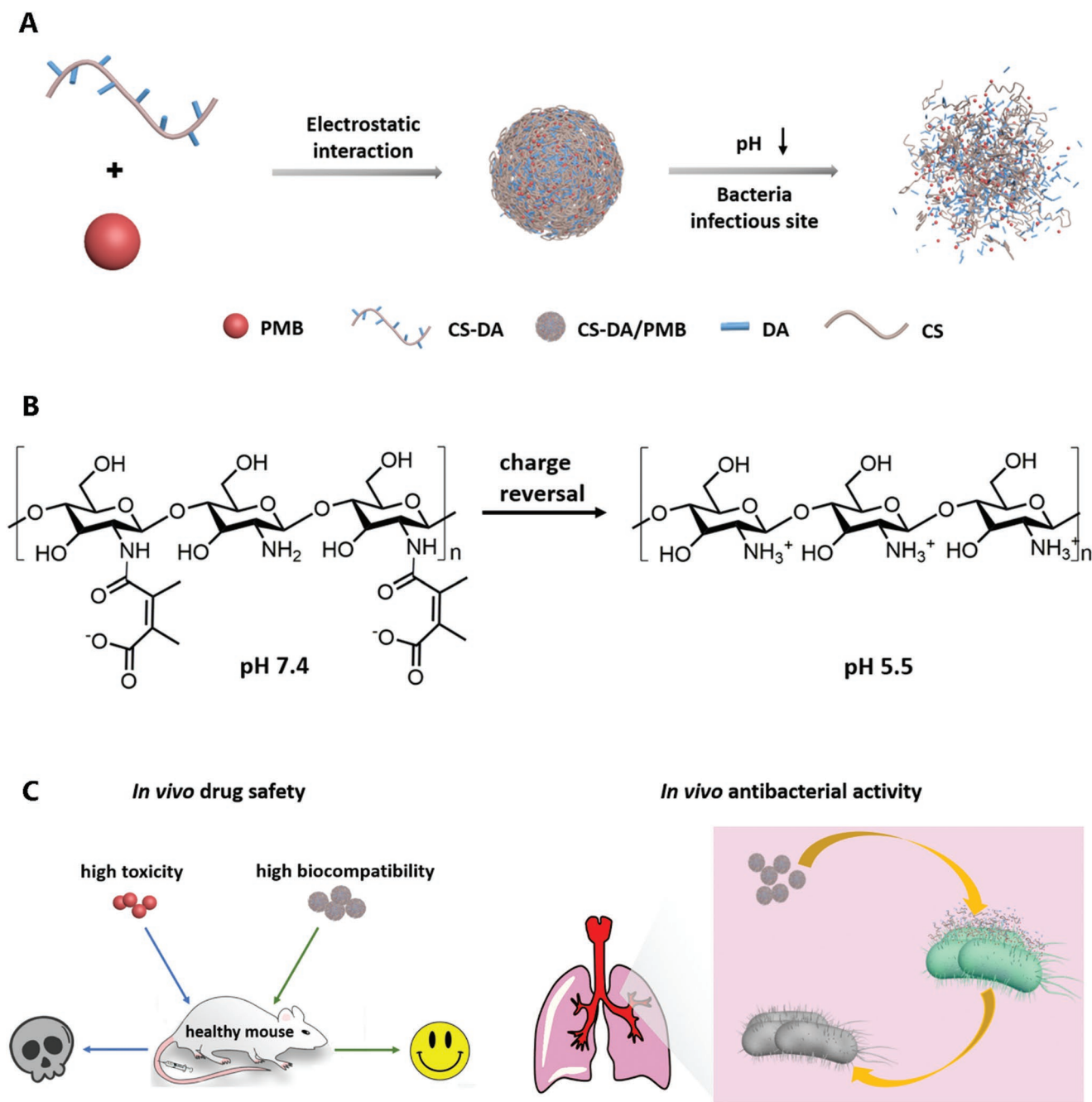
Several methods have already been used to reduce the toxicity of polymyxin

through shielding the cationic part by negative-charged derivative or reducing the number of cationic residues. For instance, polymyxin prodrugs have been synthesized through chemical modification of cationic amino acid with anion or neutral substance,^[17,18] such as methanesulfonate,^[19] PEG,^[20] etc. However, although the prodrug strategy could significantly reduce the adverse effects of polymyxin, the antibacterial activity was sacrificed due to the loss of positive charge. Alternatively, nanoparticles like liposome,^[21] silica nanoparticles,^[22] and polymeric particles,^[23,24] were developed as delivery nanoplatfroms to improve the drug safety. Despite the reduced toxicity, these nanocarriers also showed reduced bactericidal activity owing to the restricted molecular freedom and constrained access to bacterial membrane. Therefore, efficient release of polymyxin from nanoparticles is very important to maintain the excellent antibacterial performance. Based on recent researches, it can be inferred that preserving the cationic function and maintaining the uncaged molecular condition are two key considerations to retain antibacterial activity of polymyxin.^[23,25] In order to enlarge the application of polymyxin in vivo, it is urgently needed to hammer out a solution that can remarkably reduce adverse effects while retaining its fine bactericidal capability.

M. Chai, Y. Gao, J. Liu, Y. Deng, D. Hu, Dr. Q. Jin, Prof. J. Ji
MOE Key Laboratory of Macromolecule Synthesis and Functionalization of Ministry of Education
Department of Polymer Science and Engineering
Zhejiang University
Hangzhou 310027, Zhejiang Province, P. R. China
E-mail: jinqiao@zju.edu.cn

 The ORCID identification number(s) for the author(s) of this article can be found under <https://doi.org/10.1002/adhm.201901542>.

DOI: 10.1002/adhm.201901542



Scheme 1. A) Schematic illustration of preparation process of CS-DA/PMB nanocomplexes. B) Schematics of acid-activated charge reversal of CS-DA at pH 5.5. C) Schematics of *in vivo* drug safety different from free PMB and CS-DA/PMB and the mechanism of antibacterial activity of CS-DA/PMB.

Herein, we proposed a pH-sensitive polyion nanocomplex to deliver PMB for acute lung infection treatment, which was expected to exhibit reduced adverse effect without compromising intrinsic antibacterial effect. This polyion nanocomplex was prepared by mixing PMB and 2,3-dimethyl maleic anhydride (DA) grafted chitoligosaccharide (CS), exhibiting electrostatic complexation between positively charged PMB and negatively charged DA blocks at pH 7.4.^[26] However, the nanocomplex could be disassembled at the acidic environment due to the charge reversal of DA moieties from negative to

positive through the hydrolysis of the amide bond resulting in the release of PMB (**Scheme 1A**).^[27,28] It is known that the typical pH of bacterial infectious sites ranges from 5.0 to 6.5.^[29–31] The CS-DA/PMB nanocomplexes were expected to be stable in physiological environment with minimal adverse effect. Upon arriving in infectious sites,^[32] the nanocomplexes could be readily disassembled and PMB could be released, exerting antibacterial activity with minimal dose (Scheme 1B). Meanwhile chitoligosaccharide could be excreted or biodegraded *in vivo* without side effect to human bodies (Scheme 1C).^[33,34] The

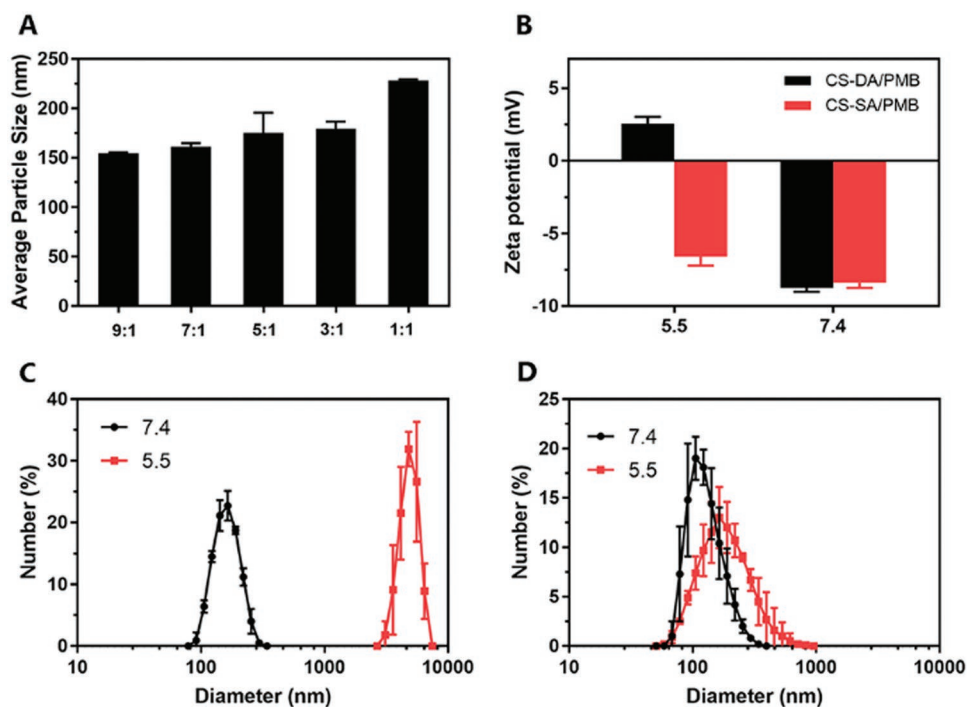


Figure 1. A) Average particle size of CS-DA/PMB nanoparticles with different weight ratios (CS-DA:PMB). B) Zeta potentials of CS-DA/PMB and CS-SA/PMB nanoparticles at pH 5.5 and pH 7.4, respectively; conversion of hydrodynamic diameter (D_h) of C) CS-DA/PMB and D) CS-SA/PMB. All data are expressed as mean \pm SD ($n = 3$ independent experiments).

CS-DA/PMB nanocomplexes were applied to treat acute lung infection caused by *P. aeruginosa* in a mouse model,^[35,36] which were expected to have potent antibacterial activity and negligible side effects in vivo (Scheme 1C).

To prepare pH-sensitive charge reversal polyion nanoparticles consisting of CS-DA and PMB, DA was grafted to CS at first. The successful synthesis of CS-DA was confirmed by ^1H NMR with the appearance of characteristic DA signals at $\delta 1.77$ and $\delta 1.74$ ($-\text{CH}_3$; Figure S1, Supporting Information). Fourier transform infrared spectroscopy (FT-IR) was used to further confirm the synthesis of CS-DA (Figure S2, Supporting Information). The peak area of wavenumber about 2700 cm^{-1} decreased obviously indicating the less amino groups. CS-SA without pH-sensitive charge reversal ability was also synthesized by the same method using succinic anhydride (SA) as control (structure determined by ^1H NMR; Figure S3, Supporting Information). Zeta potential of CS-DA and CS-SA measured in Table S1 in the Supporting Information further confirmed the successful synthesis. Then, nanocomplexes with different weight ratio were prepared by mixing CS-DA and PMB (9:1–1:1) through electrostatic interaction. The hydrodynamic size of these nanocomplexes were measured by dynamic light scattering (DLS) (Figure 1A). CS-DA/PMB nanocomplexes with weight ratio of 9:1 (CS-DA: PMB) showed smaller hydrodynamic size ($D_h = 154.2 \pm 1.4\text{ nm}$) and better stability, which were chosen for the following experiments. The CS-DA/PMB nanocomplexes had a regular and well-defined spherical morphology, detected by transmission electron microscopy (TEM) (Figure S4, Supporting Information). The charge reversal and subsequent disassembly of CS-DA/PMB nanocomplexes was studied by measuring zeta potential and hydrodynamic size after incubation at pH 5.5 for 2 h while the zeta potential of free PMB

was also detected as $+1.4 \pm 0.43\text{ mV}$ (Table S1, Supporting Information). As shown in Figure 1B, the zeta potential of CS-DA/PMB nanocomplexes changed from -8.75 to $+2.63\text{ mV}$ due to the hydrolysis of the amide bond between DA and amino group, indicating pH-triggered charge reversal. Meanwhile, the hydrodynamic size of CS-DA/PMB nanocomplexes increased to $9\text{ }\mu\text{m}$ (Figure 1C), which further supported the disassembly of nanocomplexes. The very large hydrodynamic size of nanocomplexes after disassembly might be ascribed to the electrostatic interaction of CS and 2,3-dimethyl maleic acid. However, CS-SA/PMB nanocomplexes did not show obvious change of zeta potential and hydrodynamic size after incubation at pH 5.5 (Figure 1D). Therefore, PMB could be released from CS-DA/PMB nanocomplexes at acidic infectious sites.

To evaluate the bactericidal activity of CS-DA/PMB nanocomplexes, the minimal inhibitory concentration (MIC) and minimal bactericidal concentration (MBC) were determined against two gram-negative bacterial strains of *P. aeruginosa* and *Escherichia coli* (Table 1). Compared to free PMB, CS-DA/PMB exhibited equivalent antimicrobial efficacy both in MIC ($2\text{ }\mu\text{g mL}^{-1}$) and MBC ($4\text{--}8\text{ }\mu\text{g mL}^{-1}$), which indicated that PMB could be released from CS-DA/PMB nanocomplexes and killed bacteria. Meanwhile, the MIC and MBC of CS-SA/PMB were much higher than CS-DA/PMB showing much weaker antibacterial activity, especially against *P. aeruginosa*. It was mainly because CS-SA/PMB nanocomplexes were stable in acidic infectious site and PMB molecules were restricted in nanocomplexes. The MIC and MBC of CS-DA and CS-SA without PMB were also evaluated to clarify that they did not show significant contribution to bacteriostatic or bactericidal effect. The standard plates counting assay was conducted to further confirm the

Table 1. Minimal inhibitory concentrations (MIC) and minimal bactericidal concentrations (MBC) (unit: $\mu\text{g mL}^{-1}$).

Entry	MIC [$\mu\text{g mL}^{-1}$]		MBC [$\mu\text{g mL}^{-1}$]	
	<i>P. aeruginosa</i>	<i>E. coli</i>	<i>P. aeruginosa</i>	<i>E. coli</i>
PMB	2	1	8	2
CS-DA/PMB	2	1	4	2
CS-SA/PMB	8	2	32	8
CS-DA	>1024	>1024	>1024	>1024
CS-SA	>1024	>1024	>1024	>1024

bactericidal activity of CS-DA/PMB in vitro. Sample solutions with different concentration (4, 8, and $16 \mu\text{g mL}^{-1}$) were incubated with *P. aeruginosa* suspension for 4, 8, or 12 h at pH 5.5. CS-DA/PMB showed the same antibacterial activity as free PMB, which might be ascribed to the efficient release of PMB in acidic environment. Compared to CS-SA/PMB, CS-DA/PMB exhibited stronger bactericidal capability when incubating with 4×10^8 CFU (colony forming units) *P. aeruginosa* for 8 h. Most of bacteria (>99.9%) were killed when treated with $8 \mu\text{g mL}^{-1}$ CS-DA/PMB or free PMB solution, while only half of bacteria died when treated with CS-SA/PMB at same concentration (Figure 2A). When incubation for 12 h, 99.99% of bacterial cells were killed in CS-DA/PMB group, indicating more PMB was released for enhanced antibacterial activity. The number of *P. aeruginosa* colonies was directly shown in Figure S5 in the Supporting Information.

Bacterial cells observed by scanning electron microscopy (SEM) supported the above antibacterial results in vision. As shown in Figure 2B, bacterial morphology was changed to an irregular division obviously when cells incubated with $8 \mu\text{g mL}^{-1}$ CS-DA/PMB for 8 h at pH 5.5. Moreover, CS-DA/PMB nanoparticles binding on the membrane of bacteria could also be observed under SEM since the amino groups on CS were exposed in an acidic environment to render nanoparticles interact with bacteria cells. However, $8 \mu\text{g mL}^{-1}$ CS-SA/PMB did not exhibit critical antimicrobial effect, and most of bacteria cells preserved normal morphology. Live/dead staining assay was also carried out to the antimicrobial activity of PMB nanocomplexes and free PMB (Figure 2C). Red fluorescence which represented dead bacterial cells in the CS-DA/PMB was similar to the free PMB group. Meanwhile, much weaker red fluorescence was observed in CS-SA/PMB group, indicating a stronger bactericidal capability of CS-DA/PMB over CS-SA/PMB nanocomplexes.

PMB is well known as a high toxic antibiotic.^[13] The biocompatibility of PMB after complexation with CS-DA was then studied. Free PMB exhibited hemolytic toxicity to some extent at high concentration of $1024 \mu\text{g mL}^{-1}$. However, both two PMB nanocomplexes did not display any hemolysis of mouse red cells even the concentration of PMB was as high as $1024 \mu\text{g mL}^{-1}$ (Figure 3A). The cytotoxicity of CS-DA/PMB nanocomplexes was investigated by incubation with NIH-3T3 fibroblast cells. The cell viability treated with CS-DA/PMB was higher than 75% at a very high concentration ($256 \mu\text{g mL}^{-1}$ equivalent to free PMB) while nearly 50% cells died by treating with free PMB at the same concentration (Figure 3B). These

results demonstrated that CS-DA/PMB nanoparticles could be used in vivo safely without hemolysis and cytotoxicity.

PMB can cause severe nephrotoxicity and neurotoxicity after intravenous injection in vivo. To investigate the safety of CS-DA/PMB nanocomplexes, we first tested the acute neurotoxicity by directly injecting a high concentration dose (12 mg kg^{-1} , equivalent to free PMB) of sample solutions into healthy mice. Based on the observation, mice received free PMB exhibited rapid breathing and massive twitching immediately after injection while mice received PMB nanocomplexes groups behaved as normal (Videos S1–S3, Supporting Information). Death rate was measured 24 h post injection to further clarify the safety (Figure 3C). 100% of mice survived after injection of nanocomplexes with one dose (12 mg kg^{-1} , equivalent to free PMB) in contrast of only 40% of mice injected with free PMB survived. The assessment of acute neurotoxicity certified that CS-DA/PMB nanoparticles could relieve shortness of breath, body convulsions, and even death caused by neurotoxicity which was aroused by PMB.

Then, we conducted a 3 day histological toxicity study on mice to test the nephrotoxicity of CS-DA/PMB. 8 mg kg^{-1} (equivalent to free PMB) sample solutions were injected into mice through caudal vein three times a day and lasted for 3 days. Mice were then asphyxiated and the organs were harvested at 24 h after last dosing. The nephrotoxicity and neurotoxicity of PMB nanocomplexes were evaluated by hematoxylin and eosin (H&E) staining of kidney and brain sections (Figure 3D). Compared to those treated with free PMB (protein-like precipitate filled the gaps in the renal tubules), kidneys of mice treated with either CS-DA/PMB or CS-SA/PMB displayed normal morphology which was the same as PBS group. Neuronal shrinking could be observed in the brains of mice that received free PMB in Figure 3D, and brain H&E staining of CS-DA/PMB and CS-SA/PMB groups showed less neurotoxicity to mice. All the results demonstrated that PMB nanocomplexes fabricated by electrostatic interaction could efficiently improve the biosafety of PMB with reduced nephrotoxicity and neurotoxicity. Furthermore, other organs were also stained at 24 h after last dosing and no toxicity was observed, indicating a systemic drug safety in vivo (Figure S6, Supporting Information).

In order to evaluate the antibacterial activity of PMB nanocomplexes in vivo, a *P. aeruginosa* acute lung infection model was fabricated. Before infection, nanoparticles were directly administrated into the lung of healthy mice via a catheter to investigate the histological response of the biomaterials. Two doses (8 mg kg^{-1} for each dose) of sample solutions were administrated into lung 4 h apart, respectively. 24 h after last dosing, lungs were harvested and stained with H&E. Tissue from all groups appeared normal which demonstrated that nanoparticles did not exhibit toxicity to lung (Figure S7, Supporting Information).

The antibacterial activity of CS-DA/PMB nanocomplexes against acute lung infection was then evaluated. Pathogens about 10^6 CFU were instilled into the lung directly via a catheter to construct the acute lung infection mice model (Figure 4A). Mice received two doses solution of nanoparticles (4 mg kg^{-1} equivalent to PMB) or free PMB (4 mg kg^{-1}). The first dose was instilled at the time of infection and the second was instilled 4 h postinfection. The mice were observed for 24 h after last

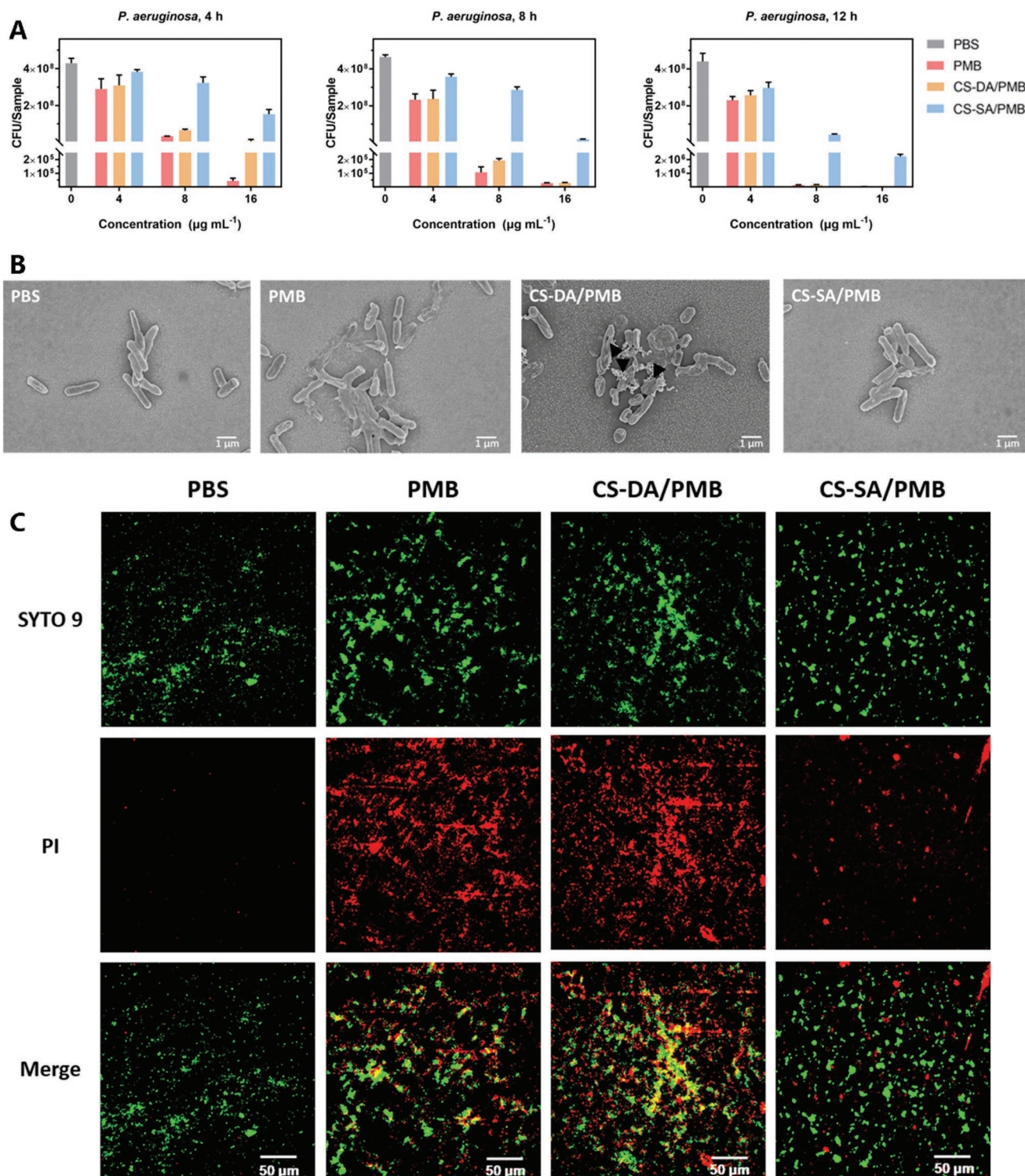


Figure 2. A) In vitro related quantitative results of standard plate counting assay. B) Morphology of *P. aeruginosa* bacteria after incubation with PBS, PMB, CS-DA/PMB, and CS-SA/PMB for 8 h characterized by SEM. Scale bar: 1 μm . C) Live/dead staining assay of *P. aeruginosa* incubated with PBS, PMB, CS-DA/PMB, and CS-SA/PMB nanoparticles, respectively. Scale bar: 50 μm . All data are shown as mean \pm SD ($n = 3$).

dosing and their lungs were harvested and photographed after they were asphyxiated. To confirm the effect of CS-DA/PMB nanoparticles, we homogenized lungs in PBS and counted the number of bacteria in them (Figure 4B; Figure S8, Supporting

Information). Treatment of mice with CS-DA/PMB caused an apparent decrease in number of bacteria comparable to free PMB due to the efficient release of PMB in acidic infectious site. Lungs treated with CS-SA/PMB still remained a relatively

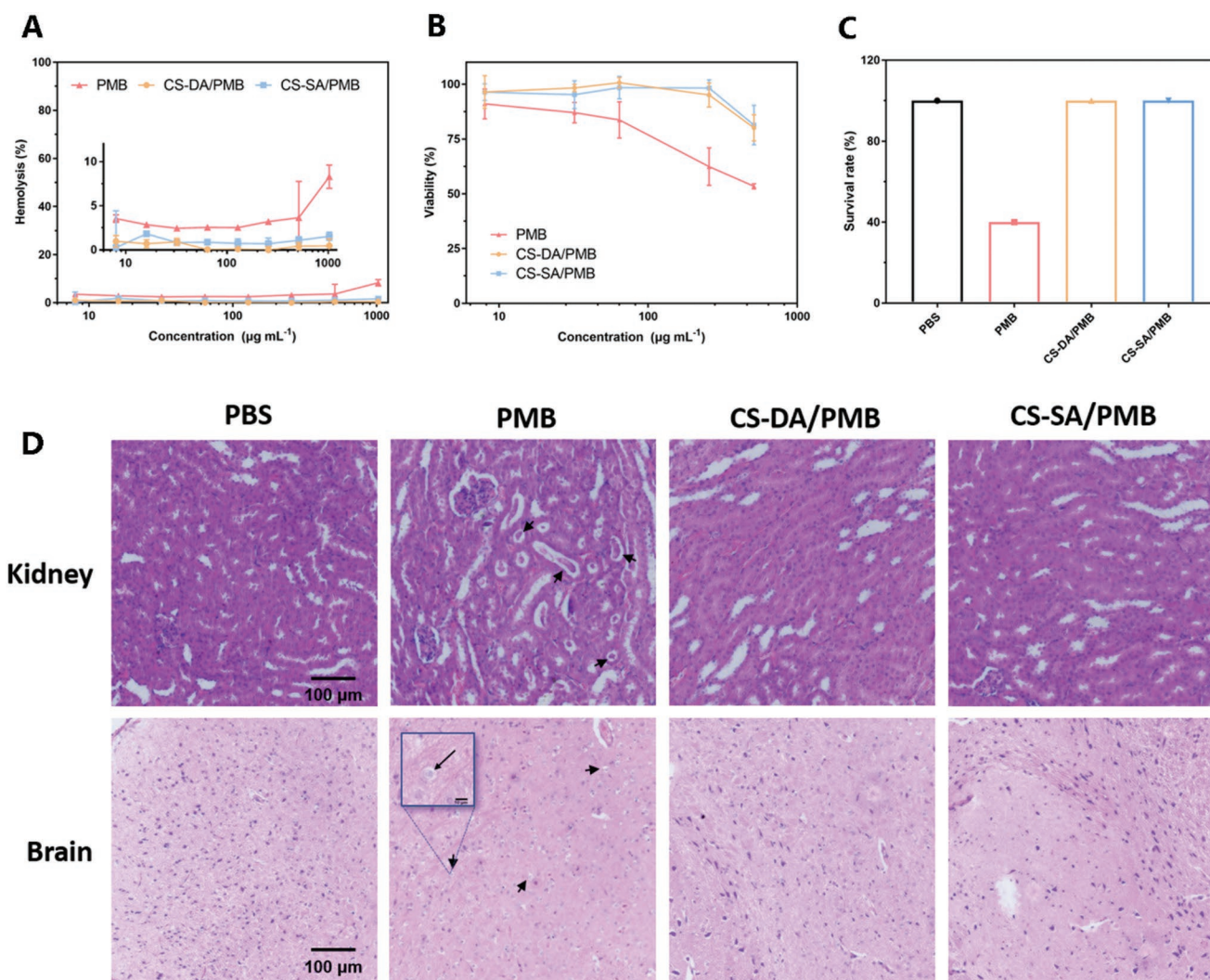


Figure 3. A) Hemolysis of mouse red cells after being incubated with PMB, CS-DA/PMB, and CS-SA/PMB with different concentrations ($n = 3$). B) Cytotoxicity of NIH-3T3 fibroblast cells after incubation with PMB, CS-DA/PMB, and CS-SA/PMB with different concentrations ($n = 3$). C) Survival rate of mice which received a high dose (12 mg kg^{-1}) of PMB, CS-DA/PMB, and CS-SA/PMB after 3 days ($n = 5$). D) H&E staining of kidneys and brains from mice which received injection of PMB, CS-DA/PMB, and CS-SA/PMB after 3 days ($n = 5$). Scale bar: $100 \mu\text{m}$ (inset scale bar: $10 \mu\text{m}$). All data are shown as mean \pm SD.

large number of pathogens ($10\text{--}11 \text{ log CFU}$). The H&E staining of lung sections were assessed at the same time (Figure 4C). The tissue sections of untreated mice in PBS group exhibited fibrosis shadow, sloughing of the bronchial epithelium, and bronchitis showing that *P. aeruginosa* caused server damage to lungs. In contrast, the normal morphology of lungs treated with CS-DA/PMB observed in tissue sections showed that these nanoparticles exhibited excellent antibacterial ability which was the same as free PMB. Moreover, the evidence of lung damage of mice treated with CS-SA/PMB showed a poor antibacterial effect of CS-SA/PMB nanoparticles. Photographs of lungs in color and morphology were consistent with the experimental results (Figure 4B).

We further investigated the antibacterial efficacy of CS-DA/PMB nanocomplexes by treatment of postinfected acute lung infection mice models (Figure 4D). Mice were administrated with $10^3 \text{ CFU } P. aeruginosa$ for 12 h to ensure that every mouse was infected, which was verified by counting the number

of bacteria in lungs. Mice were then received two doses of free PMB (4 mg kg^{-1} per dose) or nanoparticles (equivalent to 4 mg kg^{-1} of free PMB per dose). Lungs were harvested and homogenized for bacteria counting 24 h after last dose. The average log_{10} value decreased to 4 CFU with treatment of CS-DA/PMB in contrast of 8.2 CFU bacteria per lung still existed in the CS-SA/PMB group (Figure 4E; Figure S9, Supporting Information). Photographs and H&E staining of lungs further supported that the antibacterial effect of CS-DA/PMB was excellent as free PMB (Figure 4F). CS-DA/PMB exhibited excellent antibacterial activity and it might be applied to clinical treatment of *P. aeruginosa* infection with reduced nephrotoxicity and neurotoxicity.

The main purpose of this study is to improve the drug safety of PMB and maintain its excellent antimicrobial activity simultaneously. A pH-sensitive CS-DA/PMB nanocomplex was successfully fabricated based on the electrostatic combination of positively charged PMB and negatively charged CS-DA. It is

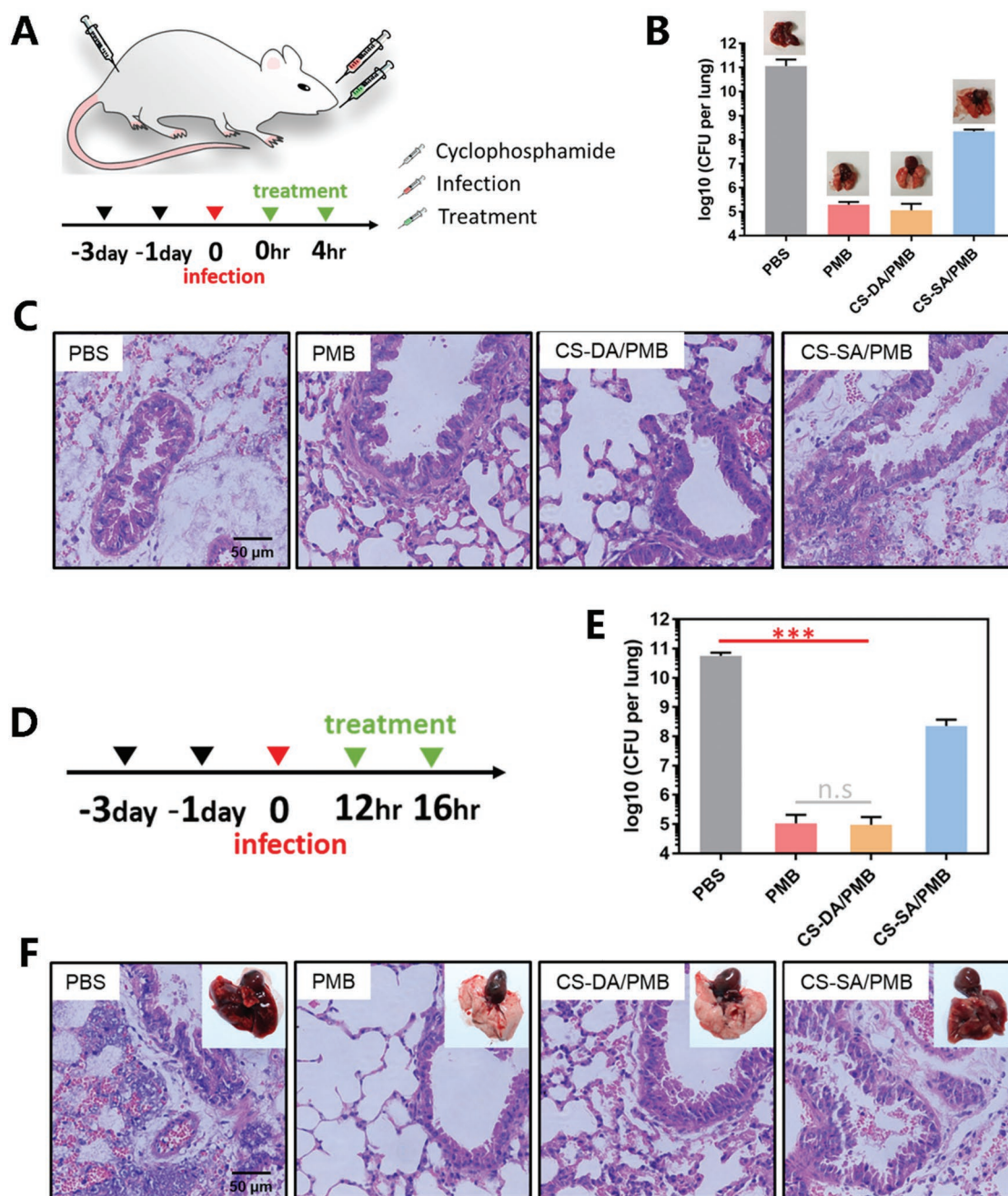


Figure 4. A) Schematic of experimental design for physiologic infection timescales of infection with *P. aeruginosa*. B) Bacterial CFU tittered from lungs of mice (infected with 10^6 CFU) treated with PBS, PMB CS-DA/PMB, and CS-SA/PMB, respectively. C) H&E staining of lungs from infective mice treated with PMB, CS-DA/PMB, and CS-SA/PMB, compared to PBS. Scale bar: 50 μ m. D) Schematic of experimental design for physiologic infection timescales of postinfection with 10^3 CFU *P. aeruginosa*. E) Bacterial CFU tittered from lungs of mice (infected with 10^3 CFU) treated with PBS, PMB CS-DA/PMB, and CS-SA/PMB, respectively. Statistical analysis was conducted using *t*-test of GraphPad Prism 6, no significance: n.s, ****P* < 0.001. F) H&E staining of lungs from infective mice treated with PBS, PMB, CS-DA/PMB, and CS-SA/PMB, respectively. Scale bar: 50 μ m. All data are shown as mean \pm SD (*n* = 6 independent experiments).

noticeable that CS-DA/PMB nanocomplexes improved the drug safety in vivo. PMB was restricted in nanoparticles when the pH value of environment was 7.4. Once they arrived at bacterial infection site, negatively charged CS-DA would convert to positively charged CS at acidic environment and PMB was released to kill the pathogens. The antimicrobial efficacy of

CS-DA/PMB nanocomplexes to gram-negative bacteria was excellent as free PMB. In mice study, nephrotoxicity and neurotoxicity caused by PMB decreased dramatically. The antibacterial activity CS-DA/PMB nanocomplexes were also observed to be same as free PMB in an acute lung infection mouse model of *P. aeruginosa*. Moreover, this method of electrostatic

combination of antibiotic and biocompatible materials could be extended to other antibiotics, thereby as a general strategy for reducing the side effects of high toxic antibiotics.

Supporting Information

Supporting Information is available from the Wiley Online Library or from the author.

Acknowledgements

This work was supported by the National Natural Science Foundation of China (51573160 and 21774110) and the Science and Technology Planning Project of Zhejiang Province (2016C04002).

Conflict of Interest

The authors declare no conflict of interest.

Keywords

biosafety, charge reversal, polyion nanocomplex, polymyxin B

Received: October 31, 2019

Revised: December 9, 2019

Published online:

- [1] M. F. Chellat, L. Raguž, R. Riedl, *Angew. Chem., Int. Ed.* **2016**, *55*, 6600.
- [2] A. Versporten, P. Zarb, I. Caniaux, M. F. Gros, N. Drapier, M. Miller, V. Jarlier, D. Nathwani, H. Goossens, *Lancet Global Health* **2018**, *6*, e619.
- [3] C. Willyard, *Nature* **2017**, *543*, 15.
- [4] D. Hu, H. Li, B. Wang, Z. Ye, W. Lei, F. Jia, Q. Jin, K.-F. Ren, J. Ji, *ACS Nano* **2017**, *11*, 9330.
- [5] K. M. O'Connell, J. T. Hodgkinson, H. F. Sore, M. Welch, G. P. Salmond, D. R. Spring, *Angew. Chem., Int. Ed.* **2013**, *52*, 10706.
- [6] M. Tumbarello, E. M. Trecarichi, A. Corona, F. G. De Rosa, M. Bassetti, C. Mussini, F. Menichetti, C. Viscoli, C. Campoli, M. Venditti, *Clin. Infect. Dis.* **2019**, *68*, 355.
- [7] R. A. Weinstein, R. Gaynes, J. R. Edwards, N. N. I. S. System, *Clin. Infect. Dis.* **2005**, *41*, 848.
- [8] M. E. Falagas, S. K. Kasiakou, L. D. Saravolatz, *Clin. Infect. Dis.* **2005**, *40*, 1333.
- [9] A. P. Zavascki, L. Z. Goldani, J. Li, R. L. Nation, *J. Antimicrob. Chemother.* **2007**, *60*, 1206.
- [10] H. Dong, Q. Xiang, Y. Gu, Z. Wang, N. G. Paterson, P. J. Stansfeld, C. He, Y. Zhang, W. Wang, C. Dong, *Nature* **2014**, *511*, 52.
- [11] A. Gallardo-Godoy, K. A. Hansford, C. Muldoon, B. Becker, A. G. Elliott, J. X. Huang, R. Pelington, M. S. Butler, M. A. Blaskovich, M. A. Cooper, *Molecules* **2019**, *24*, 553.
- [12] J. A. Justo, J. A. Bosso, *Pharmacotherapy* **2015**, *35*, 28.
- [13] K. D. Roberts, M. A. K. Azad, J. Wang, A. J. Horne, J. Li, *ACS Infect. Dis.* **2015**, *1*, 568.
- [14] T. Kelesidis, M. E. Falagas, *Expert Opin. Drug Saf.* **2015**, *14*, 1687.
- [15] T. Velkov, C. Dai, G. D. Ciccosto, R. Cappai, D. Hoyer, J. Li, *Pharmacol. Ther.* **2018**, *181*, 85.
- [16] B. Yun, M. A. Azad, J. Wang, R. L. Nation, P. E. Thompson, K. D. Roberts, T. Velkov, J. Li, *J. Antimicrob. Chemother.* **2015**, *70*, 827.
- [17] A. Gallardo-Godoy, C. Muldoon, B. Becker, A. G. Elliott, L. H. Lash, J. X. Huang, M. S. Butler, R. Pelington, A. M. Kavanagh, S. Ramu, *J. Med. Chem.* **2016**, *59*, 1068.
- [18] M. Vaara, *Med. Res. Rev.* **2018**, *38*, 1661.
- [19] S. J. Wallace, J. Li, R. L. Nation, R. J. Prankerd, T. Velkov, B. J. Boyd, *J. Phys. Chem. B* **2010**, *114*, 4836.
- [20] C. Zhu, E. K. Schneider, J. Wang, K. Kempe, P. Wilson, T. Velkov, J. Li, T. P. Davis, M. R. Whittaker, D. M. Haddleton, *J. Controlled Release* **2017**, *259*, 83.
- [21] M. Alipour, Z. E. Suntres, *Ther. Delivery* **2014**, *5*, 409.
- [22] Z. Gounani, M. A. Asadollahi, R. L. Meyer, A. Arpanaei, *Int. J. Pharm.* **2018**, *537*, 148.
- [23] Y.-H. Liu, S.-C. Kuo, B.-Y. Yao, Z.-S. Fang, Y.-T. Lee, Y.-C. Chang, T.-L. Chen, C.-M. J. Hu, *Acta Biomater.* **2018**, *82*, 133.
- [24] S. Obuobi, Z. X. Voo, M. W. Low, B. Czarny, V. Selvarajan, N. L. Ibrahim, Y. Y. Yang, P. L. R. Ee, *Adv. Healthcare Mater.* **2018**, *7*, 1701388.
- [25] I. Insua, S. Majok, A. F. Peacock, A. M. Krachler, F. Fernandez-Trillo, *Eur. Polym. J.* **2017**, *87*, 478.
- [26] Y. Li, J. Yang, B. Xu, F. Gao, W. Wang, W. Liu, *ACS Appl. Mater. Interfaces* **2015**, *7*, 8114.
- [27] E. Jin, B. Zhang, X. Sun, Z. Zhou, X. Ma, Q. Sun, J. Tang, Y. Shen, E. Van Kirk, W. J. Murdoch, *J. Am. Chem. Soc.* **2013**, *135*, 933.
- [28] B. R. Lee, K. T. Oh, Y. T. Oh, H. J. Baik, S. Y. Park, Y. S. Youn, E. S. Lee, *Chem. Commun.* **2011**, *47*, 3852.
- [29] L. G. Rahme, E. J. Stevens, S. F. Wolford, J. Shao, R. G. Tompkins, F. M. Ausubel, *Science* **1995**, *268*, 1899.
- [30] A. Riemann, A. Ihling, J. Thomas, B. Schneider, O. Thews, M. Gekle, *Biochim. Biophys. Acta, Mol. Cell Res.* **2015**, *1853*, 299.
- [31] Y. Gao, J. Wang, D. Hu, Y. Deng, T. Chen, Q. Jin, J. Ji, *Macromol. Rapid Commun.* **2019**, *40*, 1800763.
- [32] S. Azarmi, W. H. Roa, R. Löbenberg, *Adv. Drug Delivery Rev.* **2008**, *60*, 863.
- [33] T. Kean, M. Thanou, *Adv. Drug Delivery Rev.* **2010**, *62*, 3.
- [34] H. Xu, Z. Fang, W. Tian, Y. Wang, Q. Ye, L. Zhang, J. Cai, *Adv. Mater.* **2018**, *30*, 1801100.
- [35] E. J. Kwon, M. Skalak, A. Bertucci, G. Braun, F. Ricci, E. Ruoslahti, M. J. Sailor, S. N. Bhatia, *Adv. Mater.* **2017**, *29*, 1701527.
- [36] C. Y. Zhang, J. Gao, Z. Wang, *Adv. Mater.* **2018**, *30*, 1803618.